Available online at www.sciencedirect.com
ScienceDirect
European Polymer Journal 43 (2007) 2604–2611
EUROPEAN POLYMER JOURNAL
www.elsevier.com/locate/europolj

Influence of maleic anhydride-grafted EPDM and flame retardant on interfacial interaction of glass fiber reinforced PA-66

Liping Li, Bin Li *, Fei Tang

Flame Materials Molecular Design and Preparation Key Laboratory of Heilongjiang Province, College of Science, Northeast Forestry University, Harbin 150040, China

Received 14 October 2006; received in revised form 5 February 2007; accepted 6 March 2007
Available online 13 March 2007

Abstract

In this paper, the effects of melamine polyphosphate flame retardant (MPP-FR) and maleic anhydride-grafted EPDM (MA-EPDM) on the interfacial interaction of PA66/GF were investigated by means of scanning electron microscopy (SEM), dynamic mechanical analysis (DMA), differential scanning calorimetry (DSC), rheological behavior and mechanical properties. The experimental results demonstrate that MPP-FR and MA-EPDM could effectively improve interfacial interactions between the PA66 and GF. Based on SEM, good interfacial adhesion between PA66 and GF in PA66/GF/FR and PA66/GF/FR/MA-EPDM composites was observed, however, MPP-FR destroyed the PA66 matrix. DMA results show that MPP-FR increased glass transition temperature (T_g) and storage modulus, and lower tan δ, while MA-EPDM showed a little effect on them in PA66/GF/FR/MA-EPDM composite compared with PA66/GF/FR. MPP-FR made PA66 crystallization temperature and the activation energy of the macromolecular segments transport increase clearly, and enhanced crystallization degree of PA66 according to DSC results. These results demonstrate MPP-FR presented the nucleate effect for the crystallization of PA66. At the low shear rate, MPP-FR and MA-EPDM obviously enhanced apparent viscosities of the composites. This is attributed that MPP-FR improved the interfacial interaction of the composites, and MA-EPDM promoted the formation of high molecular weight structures by the reactions between MA and amine groups. All results in this paper were consistent, and showed the good interaction among PA66, GF, MPP and MA-EPDM, which were proved by the mechanical properties of the composites.

Keywords: PA66; Interfacial interaction; Morphology; Rheological behavior; Glass fiber; Flame retardant

1. Introduction

Polyamide 66 (PA66), as an engineering thermoplastic, is playing an important role in modern industrial field. However, PA66 has some disadvantages, such as poor dimensional stability, high moisture absorptivity, low heat deflection temperature (HDT) and easy flammability [1]. Reinforced plastics have achieved popularity in a short time due to design flexibility, corrosion resistance, high strength, dimensional stability, light weight, low

* Corresponding author. Fax: +86 451 8219 1571.
E-mail address: libinzh62@163.com (B. Li).

0014-3057/$ - see front matter © 2007 Elsevier Ltd. All rights reserved.
doi:10.1016/j.eurpolymj.2007.03.008

tooling and finishing lost. Glass fiber reinforced PA has become available in recent years and is used in gears, automotive industry and a variety of domestic appliances. Glass fiber reinforcement leads to a substantial increase on the tensile strength, flexural modulus, hardness, creep resistance and HDT, whereas, glass fiber reinforced PA is flammable material. In order to obtain the flame retardancy of UL94 V-0 rating, many researches have been reported in the literatures [2–5]. Some bromine containing flame retardants show very effective flame retardancy in PA. However, they have been limited in application of polymeric materials due to the corrosiveness and toxicity of products generated during the combustion process [6]. Non-halogen flame retardants have been popularly applied in PA [7,8]. Melamine cyanurate (MCA) is one of the most important non-halogen flame retardants of PA. It presents the very effective flame retardancy in non-glass fiber reinforced PA. However, it is rarely effective in the flame retardancy of glass fiber reinforced PA due to candlewick effect during burning. Red phosphorus or modified red phosphorus has been reported to be a very effective flame retardant of glass fiber reinforced PA, and glass fiber reinforced PA66 filled with red phosphorous of 5–7.5% can reach UL-94 V-0 rating. However, its application is restricted because of its color problem and highly toxic phosphine produced during processing and storing [9]. Meanwhile, owing to the poor interfacial interaction, the introduction of red phosphorus destroys the mechanical properties of glass fiber reinforced PA [10]. Melamine polyphosphate (MPP) is considered to be a favorable flame retardant of glass fiber reinforced PA66 due to high thermal stability, flame retardant efficiency, color advantage and good mechanical properties.

The ultimate mechanical properties of composites depend on the characteristics of the matrix and fibers, as well as their adhesion strength. Generally, PA66 and GF do not strongly interact with each other, resulting in poor stress transfer along the interface [5,6]. This lack has led many researchers to seek new ways to improve the adhesion characteristics of fiber/matrix interface. Botrlho et al. [11] and Idemura and Haraguchi [12] performed an in situ interfacial polycondensation of PA66 and fibers by putting fibers, adipic chloride and hexamethylenediamine together, their results show an enhanced interface compared to that of composites prepared by melt blending of PA66 and unsized fibers. Wade et al. [13] investigated the effect of plasma treatment. In fact, very few if any direct chemical bonds were created between the fibers and PA66, and the interface was not improved enough. Many researches are conducted on how to enhance the interface interaction for increasing the mechanical and physical properties of composites [14–17]. The interfacial interaction is also very important for improving mechanical properties of flame retarded and glass fiber reinforced PA66, however, the interfacial interaction is rarely reported.

Non-halogen flame retarded and glass fiber reinforced PA66 is a very important engineering plastics in electric appliances. In our contribution, the effects of MPP-FR and MA-EPDM on interfacial behavior of glass fiber reinforced PA66 composites are investigated by morphology, thermal behavior, rheological behavior, dynamic and mechanical properties.

2. Experimental

2.1. Materials

Maleic anhydride-grafted EPDM (MA-EPDM) was offered by Rizhisheng plastics company. The E-Glass Fiber (GF) treated with aminosilane coupling agent in this study was produced by Taishan Glass Fiber Limit Co., and the diameter of glass fiber is 10 μm. PA66 manufactured by Heilongjiang Engineering Plastics Company was dried at 80 °C for 24 h before use, and melamine polyphosphate (MPP) used as flame retardant was prepared by our laboratory.

2.2. Processing

All the composites in this study were prepared by melt mixing using a co-rotating 35 mm twin-screw extruder at operating temperature profiles of 220–275–275–275–275–270 °C. The components of the composites are 75% PA66 and 25% glass fiber for PA66/GF, 50% PA66, 25% GF and 25% FR for PA66/GF/FR, and 43% PA66, 25% GF, 25% FR and 7% MA-EPDM for PA66/GF/FR/EPDM, respectively. The loading of 25% MPP-FR can reach UL-94, V-0 rating, for PA66/GF composites. The extrudants were dried in a vacuum oven at 85 °C for 6 h, and were injection molded at 280 °C into various testing specimen.

2.3. Scanning electron microscopy (SEM)

For the observation of interface behavior and dispersivity of glass fibers in PA66/GF, PA66/GF/FR or PA66/GF/FR/MA-EPDM, specimens were fractured under liquid nitrogen condition. The fracture surface of the sample was sputter-coated with gold layer before examination, and the morphology micrographs of the composites were obtained at magnifications of 1000× using FEI QuanTa200 SEM (Holand), which the accelerating voltage was 15 kV.

2.4. Dynamic mechanical analysis (DMA)

Dynamic mechanical analysis was carried out by means of stress–strain oscillation measurement. Dimension of samples is 10 mm × 60 mm × 3 mm. All experiments were carried out at a frequency of 3 Hz, a heating rate of 3 °C/min, temperature range from 25 to 260 °C. The specimens were dried at 105 °C for 48 h under vacuum before testing. The viscoelastic properties, such as the storage modulus (E') and the loss factor tangent ($\tan\delta$), were measured for each sample in this temperature range as a function of temperature.

2.5. Thermal analysis

Thermal analysis tests were carried out using a Perkin–Elmer Diamond differential scanning calorimetry (DSC) apparatus. All measurements were tested under pure nitrogen gas at a heating rate of 10 °C/min. The weight of samples was kept about 5 mg. The samples were first heated from 25 to 280 °C and held at this temperature for 5 min to remove their thermal history. The samples were then cooled to 25 °C and held for 2 min before reheating to 280 °C. The values of crystallization temperature (T_c), melting temperature (T_m) and melting enthalpy (ΔH_m) were determined from the cooling and second heating scans.

2.6. Rheology measurements

The apparent viscosity of the composites was determined at 270 °C under the shear rates ranging from 10 to $10^3\ s^{-1}$ using a capillary rheometer (MLW-400) with a capillary diameter of 1 mm and L/D ratio of 40. End corrections were not applied, hence the value obtained are apparent viscosity.

2.7. Mechanical testing

Determination of tensile and flexural properties was carried out with a Regeer computer controlled mechanical instrument, and the test of Izod impact was performed by Notched Izod impact instrument, respectively, accordance to ASTM standards.

3. Results and discussion

3.1. Morphology observation

The SEM micrographs of the composites (PA66/GF, PA66/GF/FR and PA66/GF/FR/MA-EPDM) are given in Figs. 1–3, respectively. The microstructure micrographs are obtained from cryofractured surfaces of the composites. From Fig. 1, voids presented around the fibers and the fracture surface was rather smooth. Glass fibers were pulled out from the polymer matrix without leaving any sign and the fibers themselves showed a very clean surface. This result demonstrates that the interfacial adhesion between PA66 and GF was very weak due to weakly physical interaction based upon fiber break and pullout.

In Fig. 2, it was observed that interfacial interaction of PA66 and GF was improved by MPP-FR flame retardant based upon the surface of fibers, and PA66 matrix cracking took place. MPP-FR showed a good interaction in PA66/GF. Despite MPP-FR improved interfacial interaction between PA66 and GF, it destroyed the matrix strength. In Fig. 3, the rough surface on GF was also seen, and the matrix cracking was not observed. This

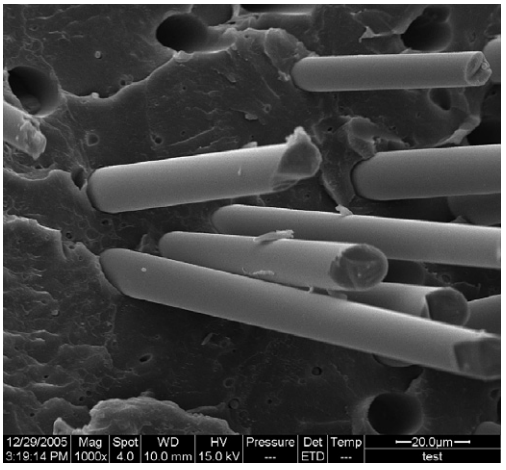

Fig. 1. SEM micrographs of PA66/GF.

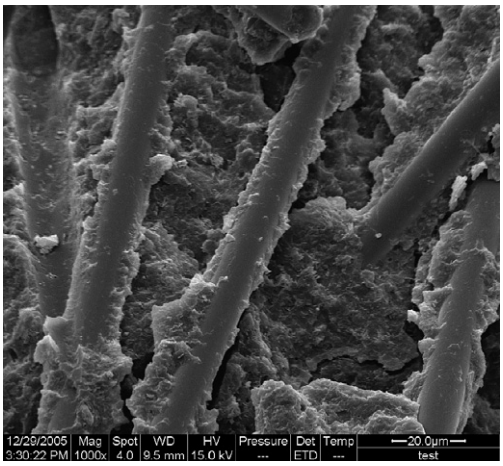

Fig. 2. SEM micrographs of PA66/GF/FR.

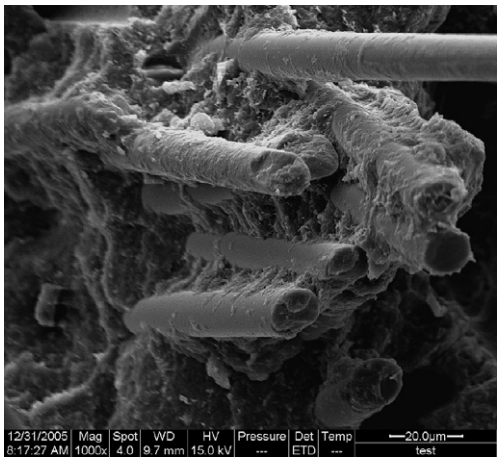

Fig. 3. SEM micrographs of PA66/GF/FR/MA-EPDM.

result demonstrates that MA-EPDM improved the interfacial interaction between PA66 and GF, and matrix toughness, proved by DMA results.

The explanation was given as following schemes. In Scheme 1, it was proposed that P–OH group in MPP-FR molecule reacted with Si–OH and $-NH_2$ on the surface of modified glass fiber to form P–O–Si bond and P–$O^-NH_3^+$–salt, and $-NH_2$ in MPP-FR could form hydrogen bonds with oxygen and nitrogen atoms in PA66 molecules. Therefore MPP-FR effectively improved the interfacial interaction between PA66 and GF. However, due to the high loading (25%) and the rigidity of MPP-FR, PA66 matrix took place the cracking while the composite was cryofractured.

Scheme 2 gave the interaction among components in the presence of MA-EPDM. It was proposed that MA groups of MA-EPDM easily reacted with Si–OH and $-NH_2$ on the glass fiber surfaces to form ester bonds and acylamide bonds, and at the same time MA groups and acylamide groups on PA66 took place the crosslinking reactions to form high molecule weight polymer chains, and the hydrogen bonds also presented in composites. So that MA-EPDM effectively improves the interfacial interaction in PA66/GF/FR/MA-EPDM composite.

3.2. DMA measurements

Polymer composites were subjected to a controlled sinusoidal strain and the resultant displacement was measured, the loss factor $\tan\delta$ versus temperature curves at 3 Hz for PA66/GF, PA66/GF/FR and PA66/GF/FR/MA-EPDM, are represented in Fig. 4.

All composites showed two damping peaks, the first peak at lower temperature was corresponding to the glass transition temperature (T_g) of PA66, which could be ascribed to the micro-Brownian motions of the matrix PA66 [18,19]. It can be used to analyze the effect of the GF and MPP-FR on this relaxation of the polymer matrix. T_g of the matrix PA66 in PA66/GF, PA66/GF/FR and PA66/GF/FR/MA-EPDM composites were 59 °C, 63 °C, 62 °C, respectively, which were obtained according to the first peak in Fig. 4. T_g of the matrix PA66 in PA66/GF is higher than that of pure PA66, which was 57 °C. This result is attributed to an effective restriction of thermally molecular motion of PA66 at the interfacial layer between PA66 and GF. With adding MPP-FR and MA-EPDM into PA66/GF composites, it was observed that peak value of $\tan\delta$ decreased and T_g increased. This result indicates that PA66 molecular chain mobility decreased at the interfacial zone, and increased the interactions between glass fiber and matrix. Ashida [20] reported that the relation between $\tan\delta$ and interface adhesion can indirectly show the interface adhesion property, and the smaller the $\tan\delta$ is, the better the interface adhesion. The experimental result is in agreement with Ashida's result. MPP-FR and MA-EPDM obviously improved the interfacial interaction between PA66 and GF, which is proved by SEM results above.

The storage modulus (E') as a function of temperature in PA66/GF, PA66/GF/FR and PA66/GF/FR/MA-EPDM system is presented in Fig. 5.

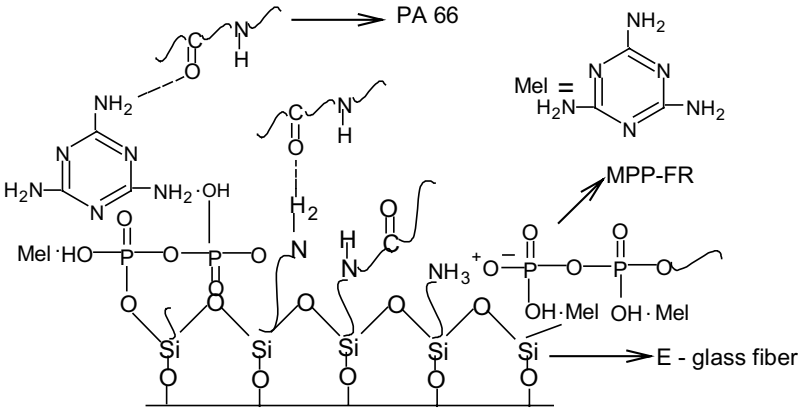

Scheme 1. Schematic hypothesis of interfacial interaction for PA66/GF/FR.

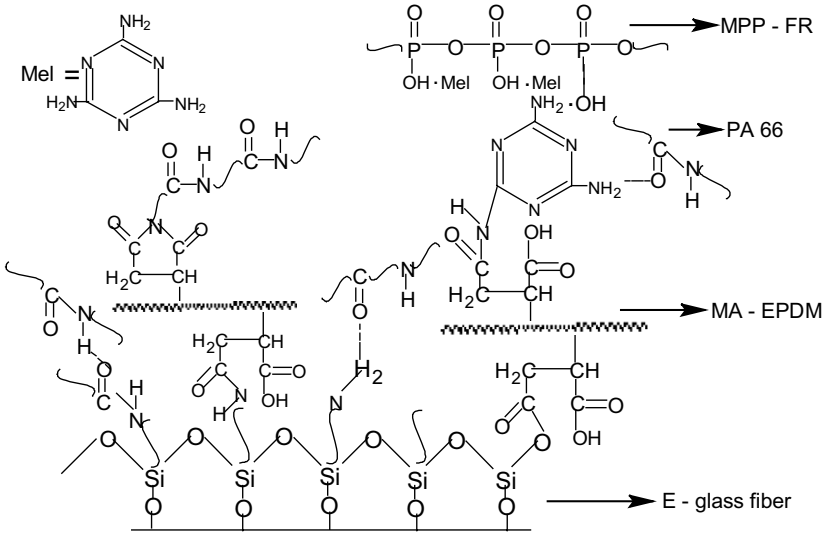

Scheme 2. Schematic hypothesis of interfacial interaction for PA66/GF/FR/MA-EPDM.

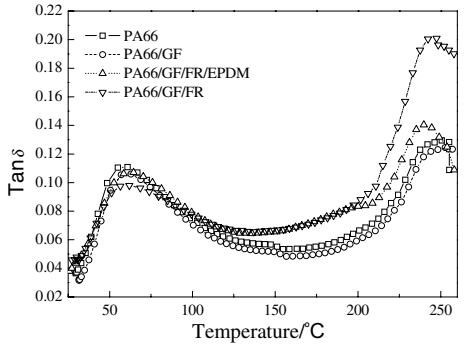

Fig. 4. tan δ of PA66 and its composites as a function of temperature.

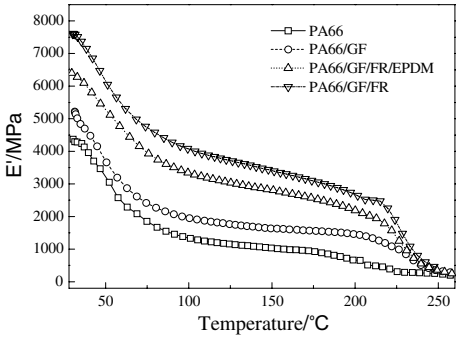

Fig. 5. E' of PA66 and its composites as a function of temperature.

From Fig. 5, MPP-FR clearly enhanced the stiffness of the composite, compared with PA66/GF composite. This result is attributed to the stronger interfacial adhesion among PA66, GF and MPP-FR, these enhanced interactions are contributed to a better stress transfer, which explains the enhanced stiffness. However, MA-EPDM decreased the stiffness of PA66/GF/FR composite according to storage modulus shown in Fig. 5. This result is attributed to MA-EPDM, a low modulus elastomer with a lower T_g, and the addition of MA-EPDM hampered the crystalline phase development of PA66. In other words, the addition of a low modulus elastomer resulted in the reduction in the storage modulus and T_g values of the composites. This result is in agreement with the SEM results discussed above.

3.3. Thermal analysis

The DSC curves of pure PA66 and its composites during cooling and heating cycles are shown in Fig. 6. It was found that two melting peaks occurred during the heating process for all PA66 composites in this study. The same observation was reported by Klein [21]. The formation of two melting peaks attributes the secondary crystallization of PA66. The thermal parameters, such as crystallization temperature (T_c), maximum melting temperature (T_m), the heat fusion (ΔH_m), the crystallinity (X_c) and crystallization activation energy (E_c), were determined or calculated from the DSC curves, which are summarized in Table 1. It was seen that the ΔH_m of PA66/GF composite was almost not affected by glass fiber. This result implied the immiscibility of the PA66 and GF. For PA66/GF/FR composite, an increase of the ΔH_m and X_c was observed, which indicated the good interaction between the PA66 and MPP-FR.

Table 1
Thermal properties of PA66 and its composites

Samples	T_m (°C)	ΔH_m[a] (J/g)	T_c (°C)	X_c[b] (%)	E_c (kJ/mol)
PA66	262.3	30.3	231.3	16.1	243.5
PA66/GF	259.5	30.4	227.0	16.2	201.1
PA66/GF/FR	261.4	35.6	235.4	18.9	305.9
PA66/GF/FR/MA-EPDM	260.8	35.1	234.2	18.7	292.5

[a] Values normalized to the amount of the PA66 phase.
[b] The X_c is calculated from the ratio of ΔH_m to ΔH_m^0, the ΔH_m^0 of PA66 with 100% degree of crystallization is 188.4 J/g [22].

As seen in Table 1, the crystallization temperatures were 231.3, 227.0, 235.4 and 234.2 °C for PA66, PA66/GF, PA66/GF/FR and PA66/GF/FR/MA-EPDM, respectively. MPP-FR caused an increase in T_c and crystallization degree (X_c) of PA66. This phenomenon is considered that MPP-FR acted as a nucleating agent, which increased the crystallization rate of PA66. This result is in agreement with that of nano-hydroxyapatite effect in PA66 by Zhang et al. [23]. In fact, in the presence of a nucleating agent, generally, it results in a reduction of the activation free energy of nucleation, however, MPP-FR increased E_c of PA66/GF/FR compared with pure PA66 and PA66/GF composite. This result was because the high addition of MPP-FR effectively improved the interface adhesion between PA66 and GF, and made the PA66 segment motion become difficult. Compared with PA66/GF/FR composite, MA-EPDM in PA66/GF/FR/MA-EPDM induced a little decrease in

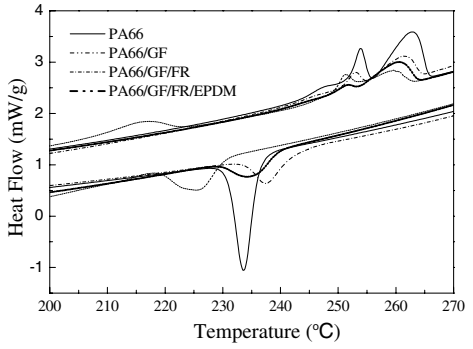

Fig. 6. DSC crystallization and melting for PA66 and its composites.

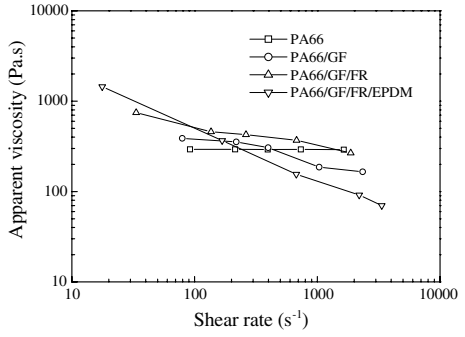

Fig. 7. The apparent viscosity measured at 270 °C for PA66 and its composites as a function of shear rate.

Table 2
Mechanical properties of PA66/GF and its composites

Sample	Tensile strength (MPa)	Flexural strength (MPa)	Flexural modulus (GPa)	Notched Izod impact strength (kJ/m^2)
PA66	82.1	110.3	2.8	5.5
PA66/GF	123.9	182.5	7.8	6.0
PA66/GF/MPP-FR	154.9	236.1	10.8	6.5
PA66/GF/FR/MA-EPDM	148.2	222.2	8.96	8.5

T_m, ΔH_m, T_c, X_c and E_c, since the PA66 molecular movement was hindered by the coupling interaction between MA-EPDM and GF or PA66.

3.4. Rheological behavior

The apparent viscosities of PA66 and its composites were measured in the capillary rheometer at 270 °C and shown in Fig. 7. The rheological behavior of the composites is generally a reflection of the change in molecular weight and the interaction among the components. From Fig. 7, the rheological behavior at 270 °C showed more distinct difference between PA66 and its composites. PA66/GF, PA66/GF/FR and PA66/GF/FR/MA-EPDM exhibited the shear thinning behavior, while the pure PA66 exhibited Newtonian fluid behavior at 270 °C. Wei also reported that the nylon 66 has the same results [24]. It is of interest that the apparent viscosities of the composites were higher than that of pure PA66, and MPP-FR and MA-EPDM obviously enhanced apparent viscosities of the composites at the low shear rate, while the apparent viscosities of the composites decreased with increasing shear rate. This result is attributed that MPP-FR enhanced the interfacial interaction strength of the composites, and MA-EPDM made high molecular weight of PA66 increase by the reactions between MA and amine groups [25,26], therefore, the motion of PA66 molecule chains were restricted.

It is noticed that the viscosities of PA66/GF/FR/MA-EPDM composite decreased sharply with increasing shear rate. Compared to PA66/GF/FR composite, MA-EPDM presented an important shear thinning behavior. The viscosity of PA66/GF/FR/MA-EPDM became very low at a high shear rate. The flow curves of the PA66/GF/FR/MA-EPDM and PA66 presented the crossover point at a shear rate of 240 s^{-1}. This crossover point has a practical significance at processing. This result is attributed to inherent property of MA-EPDM, that is, the rate of disentanglement was greater than that of entanglement at the high shear rate.

3.5. Mechanical properties

The influences of MPP-FR and MA-EPDM on the mechanical properties of PA66/GF materials are shown in Table 2. Glass fibers obviously enhanced tensile strength, flexural strength and notch Izod impact strength of PA66/GF composite. MPP-FR with a loading of 25% effectively increased mechanical properties compared with the PA66/GF composite. This result clearly proved that MPP-FR improved the interfacial interaction of the components in PA66/GF/FR composite. MA-EPDM, as an interfacial compatiblizer, is an elastomer. However, MA-EPDM with a loading of 7% was still able to keep good mechanical properties including tensile strength and flexural strength, and increased notch Izod impact strength, compared with the PA66/GF/FR composite. This result further proved that MA-EPDM was an effective interfacial compatiblizer for flame retarded and glass fiber reinforced PA66. These results of mechanical properties are in agreement with above interfacial analysis results.

4. Conclusions

The effects of MPP-FR and MA-EPDM on interfacial behavior of glass fiber reinforced PA-66 composites are discussed by SEM, DSC, DMA, rheological behavior and mechanical properties. Following conclusions can be drawn:

MPP-FR can effectively improve the interfacial interaction between PA66 and GF. MPP-FR presents a nucleate effect for the crystallization of PA66, it makes PA66 crystallization temperature and the activation energy of the macromolecular segments transport increase clearly, and enhances crystallization degree of PA66 by DSC results. The addition of MPP-FR also presents higher T_g, storage modulus and lower $\tan\delta$ of the composites.

MA-EPDM, as an interfacial compatibilizer, is used in PA66/GF/FR to improve the interfacial interaction between PA66 and GF. Based upon SEM, DMA, DSC, rheological behavior and

mechanical properties results discussed above, MA-EPDM can obviously enhance the interfacial interaction between PA66 and GF. It is proposed that these results are attributed to the chemical reactions of MA moieties on elastomers with the amine groups of PA66, and lower molecular chain mobility at the interfacial zone.

All interfacial analysis and mechanical properties obtained in this paper indicate that MPP-FR and MA-EPDM present the good interfacial interactions in PA66/GF composites.

Acknowledgments

The authors gratefully acknowledge the financial support from the project provided by Key Technologies R&D Programme of Heilongjiang province (GB03A203) and Heilongjiang Science Fund for Distinguished Young Scholars (JC04-06).

References

[1] Eccles AJ, Steele TA, Robinson AW. Appl Surf Sci 1999;106:144.
[2] Moriwaki T. Composites 1996;27:397.
[3] Van Wa beeke L, De Schryver D. US Patent 1992; 5674972.
[4] Wong SC, Nair SV, Vestergarrd LH. Plast Eng 1995:23.
[5] Hamada H, Ikuta N, Nishida N, Maekawa Z. Composites 1994;25:512.
[6] Ikuta N, Suzuki Y, Maekawa Z, Hamada H. Polymer 1993;34:2445.
[7] Jou WS, Chen KN, Chao DY, Lin CY, Yeh JT. Polym Degrad Stab 2001;74:239.
[8] Chen YH, Wang Q. Polym Degrad Stab 2006;91:2003.
[9] Davis J, Huggard M. J Vinyl Add Technol 1996;2:69.
[10] Zhang W, Bie QM, Yuan JY. Eng Plast Appl 2006;34:50.
[11] Botrlho EC, Scherbakoff N, Rezende MC, Kawamoto AM. Macromolecules 2001;34:3367.
[12] Idemura S, Haraguchi H. US Patent 2000; 6063862.
[13] Wade GA, Cantwell WJ, Pond RC. Interface Sci 2000;8:363.
[14] Hristov VN, Vasileva ST. J Appl Polym Sci 2004;97:1286.
[15] Kristiina Oksman, Craig Clemons. J Appl Polym Sci 2003;67:1503.
[16] Salehi-mobarakeh H, Brisson J, Ait-kadi A. J Mater Sci 1997;32:1297.
[17] Kazuya N, Michihiro T, Atsushi T, et al. Polymer 2002;43: 4055.
[18] David Harper, Michael Wolcott. Composites 2004;35:385.
[19] Thomason JL. Compos Sci Technol 2001;61:2007.
[20] Ashida M, Noguchi T. J Appl Polym Sci 1985;30:1011.
[21] Klein N, Seliransky D, Marom G. Polym Compos 1995;16: 189.
[22] Brandrup J, Lmmergut EH. Polymer handbook. 2nd ed. New York: Wiley-Interscience; 1975.
[23] Zhang X, Li YB, Lv GY, et al. Polym Degrad Stab 2006;91:1202.
[24] Wei F, Abdellatif Ait-kad, Josee B, et al. Polym Compos 2003;24:512.
[25] Wu DZ, Wang XD, Jin RG. Eur Polym J 2004;40:1223.
[26] Tung J, Gupt RK, Simona GP, et al. Polymer 2005;46:104.